Dear. Referee #2

We uploaded response letter for the comments of all reviewer and revised manuscript entitled, "Retrieval pseudo BRDF-adjusted surface reflectance at 440 nm from Geostationary Environmental Monitoring Spectrometer (GEMS)".

All comments of reviewers were seriously touched by authors and answered in response letter. We tried our responses can satisfy all reviewers, and our manuscript has been more improved by your advice.

Comments and Suggestions for Authors as follows (Referee 2):

1. In the abstract, "This study pioneered the application of the BRDF model to hyperspectral satellite data in the UV-VIS region, aiming to provide more realistic preliminary surface reflectance data". But in the title and the manuscript only 440nm (Page 3, Line 85) is discussed. Then how the authors can demonstrate the application to the boarder spectral range of UV-VIS?

➔ This study is designed to apply the operational algorithm for surface reflectance of GK-2B/GEMS, which observes the UV-VIS wavelength range. It is the first research to apply atmospheric correction and BRDF to an operational algorithm in this spectral range. However, due to limitations in validation data, the study was conducted at 440 nm. The intention behind the description in the manuscript is to explain the potential for future application of this method. Therefore, while this pioneering study confirms the initial feasibility of applying the algorithm, it will need to be extended to the UV wavelength range in the future.

In summary, this research is significant as it is the first to apply RTM-based atmospheric correction and BRDF modeling to derive BSR in the operational surface reflectance algorithm of environmental satellites observing the UV-VIS range. Although the analysis focused on 440 nm, we plan to extend it to the UV range.

However, we understand the point raised by the reviewer and have accordingly revised or removed some potentially overstated sentences in the manuscript as follows. (The previously written parts are in blue and italics, and the newly added/replaced parts are in red and italics.)

(Line 7-9; In Abstract)
This study pioneered the application of the BRDF model to hyperspectral satellite data at 440 nm ~~in the UV-VIS region,~~ aiming to provide more realistic preliminary surface reflectance data.

(Line 84-85; In Section 1. Introduction)
Therefore, in this study, we propose, for the first time, the application of the BRDF model to hyperspectral satellite data ~~by observing the UV-VIS region~~ for more realistic preliminary surface reflectance data.

(Line 395-396; In Section 5. Conclusion)

(Before the change)

This study introduced the novel concept of BSR as an alternative output to resolve the output precedence dilemma between land surface reflectance and other L2 outputs applied to GEMS, a hyperspectral satellite observing in the UV-VIS range.

(After the change)

This study represents the first practical application of BSR as an alternative output to resolve the output precedence dilema between land surface reflectance and other L2 outputs applied to GEMS at 440 nm, evaluating its feasibility for operational use.

(Line 425-427; In Section 5. Conclusion)

Although limitations exist, such as the challenge of capturing sudden changes in surface characteristics such as snow or ice cover, our research is pioneering in its application to BRDF modeling and evaluation in hyperspectal ~~UV-VIS~~ observation satellite studies.

2. Page 3, Line 80 “This approach reflects both the high temporal resolution of GLER and the advantages of DLER’s own BRDF”. Can you explain more what advantage of DLER is preserved?

➔ As stated in the text, GLER data is a data reproduced through inversion of LER based on MODIS BRDF data, and has the advantage of having a higher temporal resolution compared to existing LER data while considering a high BRDF. However, the wavelength produced by MODIS and the wavelength produced by GLER do not match, but because the reflectance ratio of 440 / 466 nm is used to calculate GLER at 440 nm, there is a concern that the BRDF effect is assumed to be linear with reflectivity ratio.

DLER data, similar to existing LER data, is data reproduced based on reflectivity accumulated over several years, but what differs from LER is that it takes into account the BRDF effect according to the satellite's viewing angle (VZA). Unlike GLER, which is produced based on MODIS BRDF data, DLER has the advantage of being able to individually consider BRDF effects at all calculated wavelengths. (As written in the text, TROPOMI DLER can be produced by calculating empirical coefficients for 9 viewing angle ranges and applying them.) However, like the existing traditional LER method, this is climate data that is not calculated in real time.

Therefore, the BSR proposed in this study is a product that contains both the advantages of GLER's high temporal resolution and DLER's own BRDF consideration at the wavelength to be calculated.

As you pointed out, the explanation seems insufficient. Accordingly, the advantages of DLER were explained in more detail. The modified parts are as follows: (The previously written parts are in blue and italics, and the newly added/replaced parts are in red and italics.)

(Line 70-78; Section 1. Introduction)

In addition, the Satellite Application Facility on Atmospheric Composition Monitoring (AC SAF) and the European Space Agency (ESA) provided a DLER database that considers the viewing geometry from GOME-2 (Tilstra et al., 2021) and the Tropospheric Monitoring Instrument (TROPOMI) (Tilstra et al., 2023). DLER data, similar to existing LER data, is reproduced based on reflectivity accumulated over several years. What differs from LER is that it takes into account the BRDF effect according to the satellite's viewing angles. The DLER database introduced by Tilstra et al. (2021) considers anisotropic features at various viewing angles as an advantage of polar and sun-synchronous orbit satellites. For example, GOME-2 and TROPOMI DLER calculations were performed using the regression coefficients calculated for the 5 and 9 view containers, respectively, allowing them to simulate BRDF effects influenced by the satellite's viewing angles.Therefore, unlike GLER may overlook the BRDF effects that change with wavelengths, DLER can simulate BRDF effects for all individual wavelengths. However, these data are constructed from climatology, such as the LER database, and are not updated annually but provided only once a month, making it difficult to reflect the changing land surface characteristics in real time. Additionally, there are limitations in reflecting the characteristics of indicators that change frequently with a single fixed coefficient, and it is difficult to consider the influence of other geometric conditions (such as the solar zenith angle).

3. Page 4, Line 113, "In this study, we utilized 550 nm AOD data to perform atmospheric correction." Why choose 550nm to conduct atmospheric correction if 440nm is the focus of this study?

➔ Most satellite AOD algorithms calculate the 550 nm AOD because the 550 nm wavelength is important because it is most scattered in the atmosphere and is widely used in various chemical models. Therefore, the general reference wavelength for most satellite AOD products is set to 550 nm. The 6SV RTM used to perform atmospheric correction in this study is also structured to input the AOD value at 550 nm. Therefore, the AOD at 550 nm was used as input in this study.

We acknowledged that this explanation was insufficient and additionally mentioned in the text the reason for using the AOD of 550 nm as follows. (The previously written parts are in blue and italics, and the newly added/replaced parts are in red and italics.)

(Line 110-114; In Section 2.2. Geostationary Environment Monitoring Spectrometer)

The GEMS AERAOD data provided AOD values for three wavelengths (354, 443, and 550 nm). The GEMS AOD at 443 nm shows high accuracy with a strong positive correlation coefficient (R-value) of about 0.89 and a low root mean squared error (RMSE) of 0.15 after validation with the AERONET observed AOD (Cho et al., 2023). In this study, we utilized 550 nm AOD data to perform atmospheric correction. Most satellite AOD algorithms calculate the 550 nm AOD due to its significant scattering in the atmosphere and its widespread use in various chemical models. Additionally, the 6SV RTM used for atmospheric correction in this study is designed to input the AOD value at 550 nm.

4. Page 4, Line 115, why Pandora is better?

➔ This does not mean that Pandora data is better than satellite data (such as GEMS, TROPOMI and OMPS), and when the TCO (Total Column Ozone) of GEMS, TROPOMI, and OMPS were verified

based on Pandora, the accuracy of the GEMS TCO output was similar to or slightly better than that of OMPS and TROPOMI. This was mentioned to confirm the stability of GEMS TCO data.

5. Page 6, Line 119, how the aerosol information is determined for the atmospheric transmittance? Is it fixed?

6. Page 6, Line 119, there are several transmittance variables used here, are they all defined in the same way or not? Namely whether they are for radiance or irradiance?

7. Page 6, Line 119, How the spherical albedo is defined?

➔ We think it will be easier for you to understand the answers to the three questions above if we explain them all at once. Atmospheric correction in this study can be performed based on the xap, xb, and xc coefficients calculated through 6SV RTM (Equation 1~4 in the text). To do this, input of angle components, aerosols, and atmospheric components is required, as shown in Table 1.

Therefore, in this study, the three angular components SZA, VZA, and RAA, TCO, AOD, and Terrain height were selected as atmospheric correction input variables, and the aerosol model was set to Contienetal. However, RTM-based calculations have slow calculation speeds, which limits their application to real-time operational algorithms. Therefore, we calculated the coefficients for various conditions (min, max, increment in Table 1) in advance and saved them in LUT format before using them.

So the answer to question 5 is: The Continental aerosol model in 6SV was used, and a total of 11 AODs (0.01, 0.05, 0.1, 0.15, 0.2, 0.3, 0.4, 0.6, 0.8, 1.0, 1.5) were simulated as shown in Table 1.

Additionally, atomspheric transmittance, several transmittances, spherical albedo, etc. mentioned in questions 6 and 7 are all values that can be obtained as output when input variables are entered into 6SV RTM and simulated. These calculation formulas are explained in detail in the 6SV Manual (Part1), and the formulas below are quoted from 6SV Manual Part1 (Vermote et al., 2006).

The description of the variables in the formula is as follows:

1. $S(\lambda)$: Spectral filter function, representing the filter response at a specific wavelength λ

2. E_s: Solar spectral irradiance, representing the solar radiation energy at a specific wavelengthλ

3. μ_s : Cosine of the solar zenith angle

4. $T_{gi}(\theta)$: Gas transmittance for the i-th gas, $T_g(\lambda,\theta)$ represents the transmittance by gases at λ and θ

5. $\tau(\theta)$: Optical depth, representing the optical thickness of the atmosphere or aerosols at λ and θ

6. $T_r(\theta_s)$: Rayleigh transmittance at the solar zenith angle

7. $T_a(\theta_s)$: Aerosol transmittance at the solar zenith angle

8. S^R : Spherical albedo for Rayleigh scattering

9. S^A : Spherical albedo for aerosols

10. S^T : Total spherical albedo

	DOWNWARD	UPWARD	TOTAL
Gas Trans: H_2O, O_3, CO_2, O_2 N_2O, CH_4, CO	$\frac{\int S(\lambda)\mu_s E_\lambda \prod_{i=1}^{7} Tg_i^\lambda(\theta_s)d\lambda}{\int S(\lambda)\mu_s E_\lambda d\lambda}$	$\frac{\int S(\lambda)\mu_s E_\lambda \prod_{i=1}^{7} Tg_i^\lambda(\theta_v)d\lambda}{\int S(\lambda)\mu_s E_\lambda d\lambda}$	$\frac{\int S(\lambda)\mu_s E_\lambda \prod_{i=1}^{7} Tg_i^\lambda(\theta_s,\theta_v)d\lambda}{\int S(\lambda)\mu_s E_\lambda d\lambda}$
Rayleigh transmittance. Aerosols transmittance. Total transmittance.	$\frac{\int S(\lambda)\mu_s E_\lambda T_\lambda(\theta_s)\, d\lambda}{\int S(\lambda)\mu_s E_\lambda d\lambda}$	$\frac{\int S(\lambda)\mu_s E_\lambda T_\lambda(\theta_v)\, d\lambda}{\int S(\lambda)\mu_s E_\lambda d\lambda}$	$\frac{\int S(\lambda)\mu_s E_\lambda T_\lambda(\theta_s) T_\lambda(\theta_v)\, d\lambda}{\int S(\lambda)\mu_s E_\lambda\, d\lambda}$

	Rayleigh	Aerosols	Total
Spherical albedo	$\frac{\int S(\lambda)\mu_s E_\lambda S^R d\lambda}{\int S(\lambda)\mu_s E_\lambda d\lambda}$	S^A	S^T

Fig 1. Description of the outputs in 6SV (6SV Manual Part 1; Vermote et al., 2006)

8. Page 7, Table 1, continental aerosol, how it is defined and determined? Do you use an optimization procedure to retrieve the aerosol properties, such as AOD? Do you assume a surface model when determine the aerosol properties?

➔ The Continental model utilized in this study is an aerosol model predefined within 6SV. This is a model produced by mixing three basic components: dust-like component (DUST), water-soluble component (WATE), and soot component (SOOT). The weighted averages of DUST, WATE, and SOOT in that order are 0.7 and 0.29, 0.01, respectively. Additionally, when simulating through 6SV, the land cover type was set to vegetation.

Additionally, in this study, we introduced the concept of BSR to address the retrieval paradox between surface reflectance and AOD mentioned in the introduction. Therefore, the algorithm used is not intended to independently retrieve AOD. Instead, GEMS AOD was utilized to calculate TOC as input data for simulating BSR. As a result, no additional optimization procedures were performed for AOD in this study.

9. Page 8, Line 195-202, the whole paragraph is duplicated from above!

➔ Thank you. We checked and deleted the duplicate parts.

10. Page 8, Equation 5, is there spectral dependency of those parameters?

➔ Certainly. The BRDF kernels (f1, f2; In Equation 5) used in this study were all based on the Roujean model (Roujean et al., 1992). The parameters K0, K1, and K2 in Equation 5 can be empirically derived from these f1 and f2 kernels. According to the study by Roujean et al. (1992), these parameters vary depending on the Earth's surface and the observed wavelength. For example, the K2 parameter can be about 3 to 5 times larger in the near-infrared than in the visible range.

Therefore, while the values at a specific point in the same channel remain almost unchanged, reflectance values vary with different channels, indicating that these variables change with the spectrum.

[Reference #1]

Roujean, J. L., Leroy, M., & Deschamps, P. Y. (1992). A bidirectional reflectance model of the Earth's surface for the correction of remote sensing data. Journal of Geophysical Research: Atmospheres, 97(D18), 20455-20468.

11. Page 8, Line 207, how time frame matters here?

➔ In BRDF modeling, the temporal variable is extremely important and can be described as the compositing period in BRDF modeling. As the compositing period lengthens, the number of available pixels increases, leading to a higher sample size for BRDF modeling and thus achieving more accurate BRDF modeling. However, a longer compositing period may overlook the reflectance distribution characteristics due to real-time changes in the surface. Therefore, the compositing period for BRDF is selected by considering the number of samples available based on the satellite's revisit cycle and the resulting accuracy of BRDF modeling. In this study, the compositing period was empirically set to 15 days.

12. Page 10, Line 231, what is the age variable? Where is it in the equation?

➔ To address the gaps that may occur due to insufficient observations during BRDF modeling, we implemented an additional design where BRDF parameters from up to 5 days prior are used when current parameters are not available for the same pixel. We defined and utilized an "Age" variable, which indicates how many days old the BRDF parameters used for gap-filling are. For instance, if BRDF parameters from 3 days ago are used, the Age variable is assigned a value of 3. If the next day also lacks newly calculated BRDF parameters and uses the same date's BRDF parameters, the Age variable is assigned a value of 4. Conversely, if new BRDF parameters are calculated, the Age variable is reset to 0. When the Age variable reaches 5, the parameters are no longer used.

We acknowledged that this explanation was insufficient and additionally mentioned in the text the reason for using the “Age” variable as follows. (The previously written parts are in blue and italics, and the newly added/replaced parts are in red and italics.)

(Line 217-221; In Section 3.2. BSR retrieval through BRDF modeling)

Insufficient observations lead to uncalculated BRDF parameters, resulting in missing BSR values, which are crucial for other L2 algorithms. To address this, a gap-filling process was implemented, utilizing the "Age" variable in BRDF modeling. This method uses previously calculated BRDF parameters up to 5 days of age to fill gaps when current parameters are unavailable. In this process, the Age variable was defined and utilized, indicating how many days old the BRDF parameters used for gap-filling are. For example, if BRDF parameters from 3 days ago are used, the Age variable is

assigned a value of 3. If the next day also BRDF parameters are not be calculated, and uses the same date's BRDF parameters, the Age variable is assigned a value of 4. Conversely, if new BRDF parameters are calculated, the Age variable is reset to 0. If the Age variable exceeds 5, the parameters are no longer used. To summarize, the Age variable indicates the number of days since the last valid BRDF calculation, reset to 0 after 5 days, or upon the BRDF parameter is calculated. ~~*calculation.*~~

13. Page 10, Line 246, "The GK-2A AMI albedo output establishes the standard for good quality BSR, requiring seven or more observations and a BRDF RMSE of 0.07 or lower" How the number of observations impact accuracy? Does this relate to the coverage of the angular range of the BRDF? Is the geometry limited for a geostationary satellite?

➔ The accuracy of BRDF modeling is influenced by the number of observations, errors in surface reflectance (TOC), and the sampling conditions of the sun-satellite angles (such as SZA and VZA). When the number of observations is low, errors in surface reflectance can be mistakenly simulated as BRDF effects. Therefore, a sufficient number of observations is essential for error reduction and stable BRDF effect simulation.

Additionally, as you mentioned, geostationary satellites like GEMS, unlike polar-orbiting satellites, exhibit significant variability in observed solar zenith angles while having minimal changes in satellite (viewing) zenith angles. This can lead to greater errors in BRDF inversion studies for conditions that are not sampled. However, this study performs BRDF modeling based on the angle components sampled by the GEMS satellite, and therefore does not consider the accuracy of BRDF at unsampled angles.

Therefore, we extracted BSR good quality pixels based on the quality flag (number of observations) applied to the AMI satellite, which observes similar angles to the geostationary GEMS satellite, and the BRDF good quality criteria (BRDF RMSE) provided by the MODIS satellite.

14. Page 11, Figure 3 shows good agreement. How does the comparison relate to solar geometry? Do you have examples what the BRDF looks like?

➔ The BRDF models used in this study are based on the Roujean BRDF model (Roujean et al., 1992), and the formulas for the two kernels (f1, f2) are as follows. Consequently, as the solar or viewing geometry changes, the reflectance changes according to the formulas below. Additionally, the two kernel values of the Roujean BRDF model show the distribution of values according to SZA and RAA (VZA = 50), as illustrated in Figures 2 and 3 below.

$$f_1(\theta_s, \theta_v, \phi) = \frac{1}{2\pi}[(\pi - \phi)\cos\phi + \sin\phi]\tan\theta_s \tan\theta_v - \frac{1}{\pi}\left(\tan\theta_v + \tan\theta_s + \sqrt{\tan^2\theta_v + \tan^2\theta_s - 2\tan\theta_s\tan\theta_v\cos\phi}\right) \quad (1)$$

$$f_2(\theta_s, \theta_v, \phi) = \frac{4}{3\pi}\cdot\frac{1}{\cos\theta_s + \cos\theta_v}\left[\left(\frac{\pi}{2} - \zeta\right)\cos\zeta + \sin\zeta\right] - \frac{1}{3} \quad (2)$$

$$\zeta = \arccos\left[\cos\theta_v\cos\theta_s + \sin\theta_v\sin\theta_s\cos\phi\right] \quad (3)$$

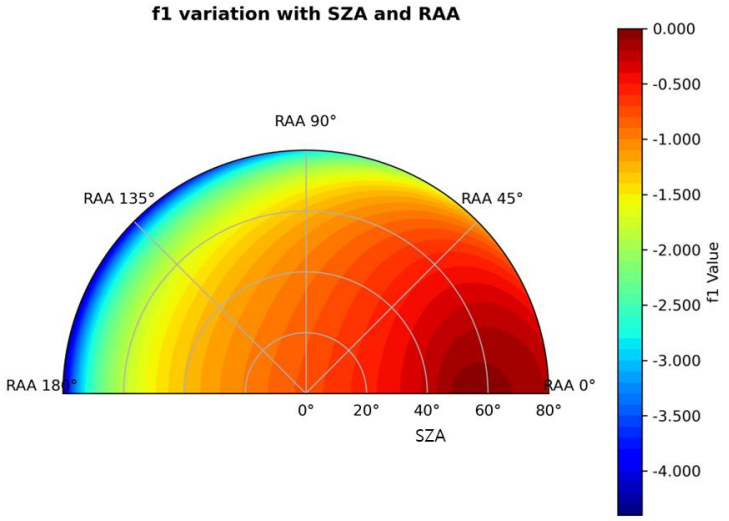

Fig 2. Roujean BRDF geometric kernel (f1) variation with SZA and RAA (VZA = 50)

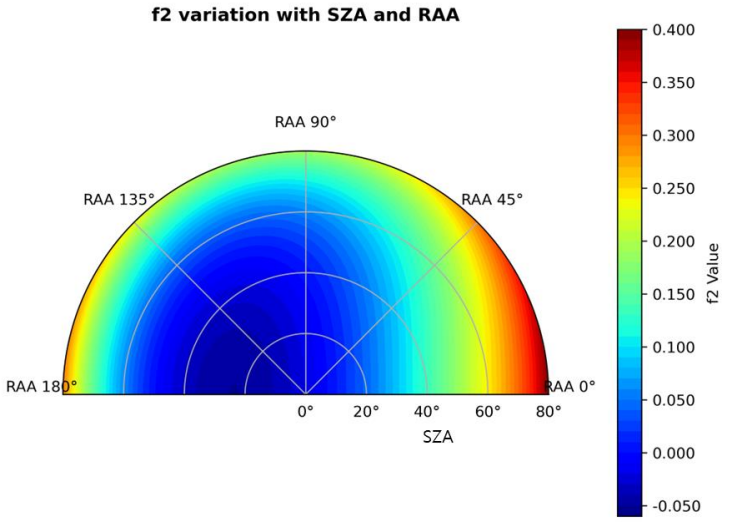

Fig 3. Roujean BRDF volumetric kernel (f2) variation with SZA and RAA (VZA = 50)

15. Page 13, Figure 4, what is the solar and view geometry here?

➔ TOC and BSR utilized solar and viewing geometry at the time of actual observation (L1C data), and LER was calculated using the minimum reflectance method and did not consider geometry separately.

16. Page 13, Line 296, how you separate the four land types? Could you show them in a map?

➔ The analysis was conducted based on MODIS land cover data. The data used is from the MODIS/Terra+Aqua Land Cover Type Yearly L3 Global 0.05Deg CMG V061 (MCD12C1), specifically from the year 2021. Figure 2 below represents the land cover according to the IGBP

classification within the MODIS Land Cover data. The values for the four land cover types used in this study (Grassland, Cropland, Shrubland and Urban) are displayed in Figure 3. The average values for all four land cover types were utilized.

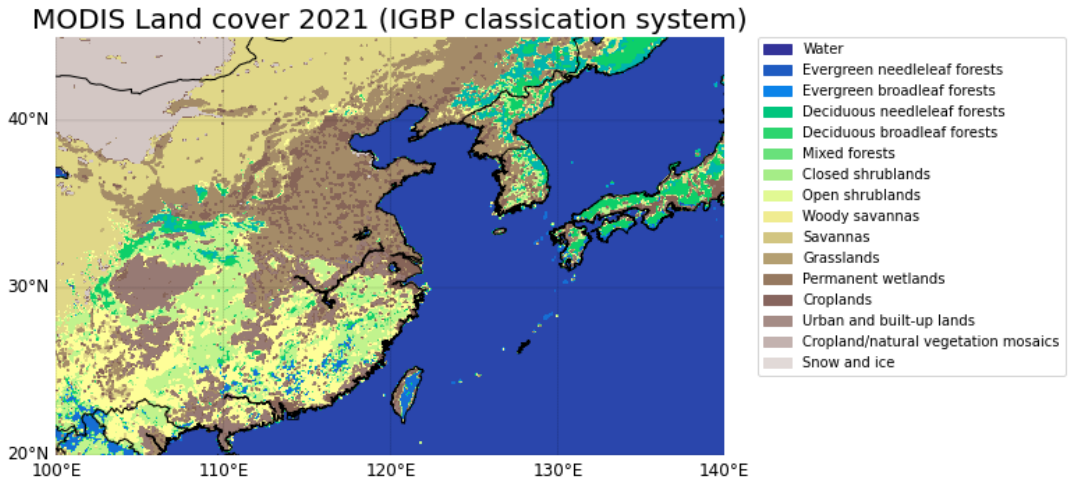

Fig 4. MODIS Landcover (IGBP classification system; 2021)

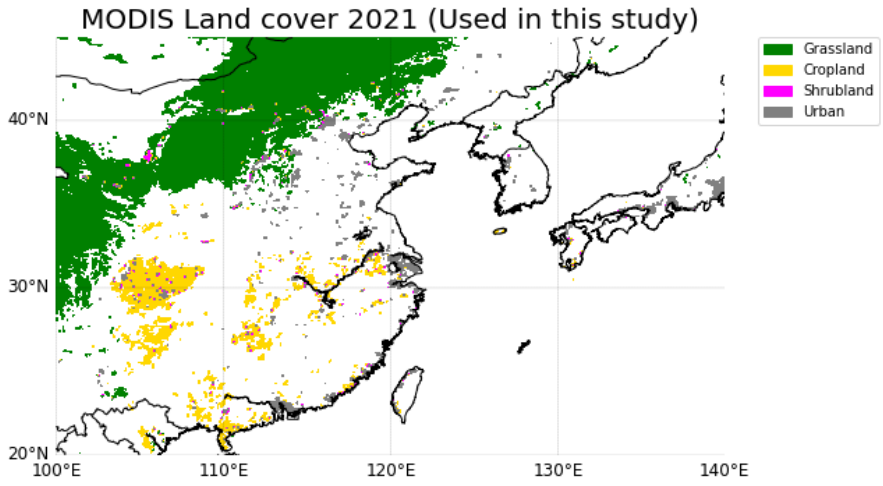

Fig 5. The area within the MODIS land cover used in this study (Grassland, Cropland, Shurbland, Urban)

17. Page 15, Line 312, how AOD is determined??

➔ The section (4.2.2.) does not involve calculating the actual AOD and performing analysis, but rather, the analysis is based on the changes in AOD according to the variations in blue channel surface reflectance presented in the study by Li et al., (2012). Using TOC reflectance as a reference value, we utilized BSR and LER as alternative reflectances. We then evaluated the potential errors in AOD estimation by creating a regression equation based on the changes presented in Table 2 of the Li et al. study.

Please refer to the paper mentioned below for further details.

[Reference #2]

Li, S., Chen, L., Tao, J., Han, D., Wang, Z., Su, L., ... & Yu, C. (2012). Retrieval of aerosol optical depth over bright targets in the urban areas of North China during winter. Science China Earth Sciences, 55, 1545-1553.

18. Page 16, Line 398, how the surface reflectance is observed from ground site? What is the spatial coverage? Any particular viewing geometry the reflectance is defined?

➔ In this study, surface reflectance at the Baotou Sandy Site (BSCN) of RadCalNet, a desert area with minimal reflectance variability. Surface reflectance at the Baotou ground site is measured using an automated observation system developed by the Academy of Opto-Electronics (AOE) at the Chinese Academy of Sciences (CAS). The system includes CR-250 spectrometers, which cover a spectral range of 380 nm to 1080 nm with a 2 nm resolution and a 3-degree field of view.

The spatial coverage for the sandy site at Baotou is 300 × 300 meters (center coordinates: 40.8658 N, 109.6155 E), with a spatial heterogeneity of less than 2.5% from 618 nm to 868 nm. Observations are made every 2 minutes from 08:30 to 17:30 local time, and the data is transferred to the data center in Beijing via the internet.

19. Page 17, Figure 7, it seems the surface reflectance variability is quite narrow comparing with the one derived from satellite. Is this because the ground site covers a small spatial range, while satellite measures a larger range?

➔ Yes, that's correct. Although the RadCalNet BSCN site is a desert area with relatively consistent reflectance distribution, its spatial coverage is only 0.3 x 0.3 km, which is significantly smaller compared to satellite observations (GEMS: 7 x 8 km at Seoul, TROPOMI: 0.125 x 0.125 degrees, OMI: 7 x 7 km at nadir). Consequently, the reflectance characteristics from areas around the site, which are not desert, are also included, leading to greater variability in the values compared to those observed at the BSCN site. Please refer to sections 2.3 and 2.4 of the QA4EO-WGCV-RadCalNet-BTCN-Q-v3.pdf linked below for photos of the BSCN site and its surroundings.

In addition, data from the time zone closest to the ground observation was used for verification. However, differences may occur due to the sun-target and target-sensor geometry characteristics inherent in satellite observation.

(URL : https://www.radcalnet.org/#!/sites/BTCN)

20. Page 20, line 396, “This study introduced the novel concept of BSR as an alternative output to resolve the output precedence dilemma between land surface reflectance and other L2 outputs applied to GEMS, a hyperspectral satellite observing in the UV-VIS range. “ Again, this study only discuss one wavelength, so the conclusion to the application to UV-VIS may be not complete.

➔ The response to this question is the same as for question 1; therefore, a separate answer was not included. We greatly appreciate the reviewer's comments and have made the necessary revisions. The updated section is included below. (The previously written parts are in blue and italics, and the newly added/replaced parts are in red and italics)

(Line 395-396; In Section 5. Conclusion)

(Before the change)

This study introduced the novel concept of BSR as an alternative output to resolve the output precedence dilemma between land surface reflectance and other L2 outputs applied to GEMS, a hyperspectral satellite observing in the UV-VIS range.

(After the change)

This study represents the first practical application of BSR as an alternative output to resolve the output precedence dilema between land surface reflectance and other L2 outputs applied to GEMS at 440 nm, evaluating its feasibility for operational use.

21. Page 21, line 404, “The simulation performance of the GEMS BSR was 3% more accurate than that of the GEMS LER data in terms of the rRMSE over the entire study period based on TOC”. Is 3% significant? How does this compare with the measurement uncertainty from GEMS?

➔ As mentioned in the introduction, the underestimation of surface reflectivity that occurs when LER based on the minimum reflectivity method is used as an alternative reflectivity directly leads to the overestimation of AOD and affects other L2 products such as clouds and gas products (NO2, SO2).

As noted in section 4.2.2, "Surface Reflectance Influence on AOD Variability in Cropland and Urban Areas," while the numerical improvement in overall accuracy is approximately 3%, the influence on AOD shows that BSR is up to about 10% better than LER, particularly in downtown areas during winter.

Therefore, the improvement of BSR is meaningful in this respect as it can address the inherent problems of LER.